Souvik Chakraborty
Department of Civil Engineering,
Indian Institute of Technology Roorkee,
Roorkee 247667, India
e-mail: csouvik41@gmail.com

Tanmoy Chatterjee
Department of Civil Engineering,
Indian Institute of Technology Roorkee,
Roorkee 247667, India
e-mail: tanmoydce88@gmail.com

Rajib Chowdhury
Department of Civil Engineering,
Indian Institute of Technology Roorkee,
Roorkee 247667, India
e-mail: rajibfce@iitr.ac.in

Sondipon Adhikari
Professor
College of Engineering,
Swansea University,
Bay Campus, Fabian Way,
Swansea SA18EN, UK
e-mail: s.adhikari@swansea.ac.uk

Robust Design Optimization for Crashworthiness of Vehicle Side Impact

Optimization for crashworthiness is of vast importance in automobile industry. Recent advancement in computational prowess has enabled researchers and design engineers to address vehicle crashworthiness, resulting in reduction of cost and time for new product development. However, a deterministic optimum design often resides at the boundary of failure domain, leaving little or no room for modeling imperfections, parameter uncertainties, and/or human error. In this study, an operational model-based robust design optimization (RDO) scheme has been developed for designing crashworthiness of vehicle against side impact. Within this framework, differential evolution algorithm (DEA) has been coupled with polynomial correlated function expansion (PCFE). An adaptive framework for determining the optimum basis order in PCFE has also been presented. It is argued that the coupled DEA–PCFE is more efficient and accurate, as compared to conventional techniques. For RDO of vehicle against side impact, minimization of the weight and lower rib deflection of the vehicle are considered to be the primary design objectives. Case studies by providing various emphases on the two objectives have also been performed. For all the cases, DEA–PCFE is found to yield highly accurate results.
[DOI: 10.1115/1.4035439]

1 Introduction

Investigating the crashworthiness of vehicle to ensure occupant safety and structural integrity is one of the main focuses of automobile industries [1]. Over the last decade, the exponential increase in computational prowess has favored the development of high-fidelity finite element analysis (FEA)-based optimization techniques to tackle industrial problems such as crashworthiness of vehicle [2–9]. However, optimum design often resides in the boundary of system failure, leaving very little or no room for modeling imperfections [10–12], parameter uncertainties [12,13], and/or human error. To overcome this issue, it is necessary to consider the effect of uncertainty in the optimization process. In literature, there exist two distinct approaches, namely robust design optimization (RDO) [14–16] and reliability-based design optimization (RBDO) [17–19], that incorporate uncertainty into the framework of optimization. While the former minimizes the propagation of uncertainty from input to the output, the latter seeks some safety measures against failure defined using a limit-state function. In this study, the main focus is on RDO, and hence, RBDO will not be discussed. Interested readers may refer [9,17–20] for details regarding RBDO.

The concept of RDO is in existence since 1920 when Fisher and Yates developed the design of experiments to improve the yield of crops in the United Kingdom. However, it was Taguchi who formally developed the foundation of robust design. Over the last decade, RDO has gained vast popularities in the field of aerospace engineering [21,22], automotive engineering [23], marine engineering [24], and civil engineering [25,26].

The concern regarding the accuracy and efficiency of existing RDO techniques is mainly twofold. First, most of the methods for RDO utilize gradient-based optimization (GBO). Although easy to implement, GBO often yields the local optima. Alternatively, if explicit expression for objective function is not available, the gradient of objective function is calculated by employing finite difference method. This renders the optimization process computationally expensive. Second, the process of uncertainty quantification is computationally intensive and often requires a tradeoff between efficiency and accuracy. Even the popular methods for uncertainty quantification such as perturbation method [27,28], Kriging [29–34], polynomial chaos expansion (PCE) [35–42], moving least square method [43–46], collocation-based approaches [47], tensor product-based approach [48], and radial basis function [49–53] often yields erroneous results when coupled into the framework of RDO. In this context, there is a need of efficient uncertainty quantification tool that can be utilized for solving RDO problems.

Recently, a new operational model, referred to as polynomial correlated function expansion (PCFE) [54–62], has been proposed for uncertainty quantification. As already demonstrated, PCFE yields highly accurate results [54–60]. In this paper, a coupled framework that couples PCFE into the framework of differential evolution algorithm (DEA) [63,64] has been utilized for RDO of vehicle due to side impact. It is argued that the coupled DEA–PCFE is efficient as well as accurate due to the following factors:

- DEA is a global optimization tool and does not yield the local minima. Moreover, it has already been established in previous studies that DEA has a rapid convergence rate [63–66].
- DEA is a gradient-free optimization technique. Therefore, it is equally applicable to both differentiable and nondifferentiable functions.
- PCFE is an efficient uncertainty quantification tool capable of dealing with high-dimensional problems. Thus, using PCFE to reconstruct the objective function and constraints makes the procedure efficient.

The primary focus of this work is to investigate the applicability of DEA–PCFE for solving the crashworthiness of a vehicle due to side impact. The novelty of this work is mainly threefold:

- PCFE is a novel operational model and has never been utilized for solving RDO problems. This is the first instance where PCFE has been utilized in RDO.
- All the existing works carried out on PCFE selects the order of basis empirically. In this paper, a guideline for determining the optimum basis order has been proposed.

Manuscript received November 18, 2015; final manuscript received October 18, 2016; published online June 12, 2017. Assoc. Editor: Sankaran Mahadevan.

- The newly proposed method is applied to a finite-element model with 1.7 million (M) nodes. Neither DEA nor PCFE have been applied to such a large-scale real-life problem. This application will give further confidence to the readers/users of this method, which has not been reported before.

The rest of the paper is organized as follows. In Sec. 2, a brief description of RDO has been provided. The concepts of DEA–PCFE are briefly reviewed in Sec. 3. In Sec. 4, results obtained using DEA–PCFE has been validated against five popular RDO techniques. The problem description along with results obtained has been discussed in Sec. 5. Finally, Sec. 6 provides the concluding remarks.

2 Fundamentals of Robust Design Optimization

Unlike conventional deterministic design optimization which do not account for uncertainties, a RDO problem develops a solution that is least sensitive to variations of the nominal design. Thus, the goal of RDO is to minimize the effects of uncertainties involved in system design without suppressing their causes [15]. To further illustrate the methodology, Fig. 1 has been presented. Of the two optimal solutions indicated by x_1 and x_2, x_2 is considered to be more robust and useful in design practice as compared to that of x_1, in spite of the latter being better as an optimal solution in mean sense. This is primarily due to the fact that at x_2 the variation in design variable does not affect the objective function $f(x)$ much or happens to be less sensitive and at the same time, maintaining the solution within the feasible region.

Several past works [15,67–70] have assigned different types of interpretations to RDO depending on the application and uncertainty quantification and hence attracted various forms of problem formulation. A summary of the same has been provided below:

(1) Minimization of the mean of objective function while constraining to a predefined level as illustrated by the below equation

$$\begin{aligned} &\min \mu(f(\mathbf{x})) \\ &\text{s.t. } \mathbf{x}_L \le \mathbf{x} \le \mathbf{x}_U \end{aligned} \tag{1}$$

where $\mu(f(\mathbf{x}))$ denotes the mean value of objective function and $\mathbf{x}_L$ and $\mathbf{x}_U$ represent the lower and upper bounds of the design variable $\mathbf{x}$. Here, the objective function represents a general loss in performance, and hence, the expected value of the same can be considered as a risk that is at par with Bayesian approach in statistical decision theory [71].

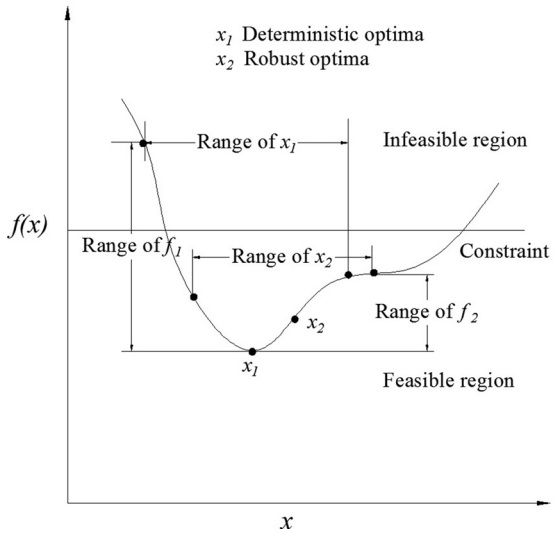

Fig. 1 Comparison of RDO with that of deterministic design optimization

(2) Minimization of the standard deviation (SD) of objective function pertaining to usual constraints as illustrated by the below equation

$$\begin{aligned} &\min \sigma(f(\mathbf{x})) \\ &\text{s.t. } \mathbf{x}_L \le \mathbf{x} \le \mathbf{x}_U \end{aligned} \tag{2}$$

where $\sigma(f(\mathbf{x}))$ denotes the standard deviation of objective function and $\mathbf{x}_L$ and $\mathbf{x}_U$ represent the lower and upper bounds of the design variable $\mathbf{x}$. This design leads to robustness in a strict sense with minimum sensitivity with respect to the variation of the probabilistic parameters [72].

(3) Multiobjective optimization by minimizing the objectives mentioned in Eqs. (1) and (2) as illustrated by the below equation [15,73]

$$\begin{aligned} &\min[\mu(f(\mathbf{x})), \sigma(f(\mathbf{x}))] \\ &\text{s.t. } \mathbf{x}_L \le \mathbf{x} \le \mathbf{x}_U \end{aligned} \tag{3}$$

However, concurrent optimization of mean and standard deviation has been observed to conflict with each other. In order to overcome this problem, the objective functions can be combined into a single robust objective function assigning relevant weightages to each of the respective functions [68] as

$$\begin{aligned} &\min \beta \frac{\mu(f(\mathbf{x}))}{\mu^*} + (1-\beta)\frac{\sigma(f(\mathbf{x}))}{\sigma^*}, \quad 0 \le \beta \le 1 \\ &\text{s.t. } \mathbf{x}_L \le \mathbf{x} \le \mathbf{x}_U \end{aligned} \tag{4}$$

where the weighing factor β represents the relative importance of the two objectives. μ^* and σ^* are the outcomes of ideal design. In this study, objective function of the form described in Eq. (4) has been considered.

3 Robust Design Optimization Using Differential Evolution Algorithm–Polynominal Correlated Function Expansion

In this section, DEA and PCFE have been reviewed. Pseudocode for PCFE has also been provided. Toward the end of this section, a flowchart depicting the coupled framework has been provided.

3.1 Differential Evolution Algorithm. DEA [63,64] is a stochastic direct search method that optimizes a problem by iteratively trying to improve a candidate solution with respect to a given measure of quality. Unlike GBO, DEA does not use the gradient of the problem and is thus equally applicable to both differentiable and nondifferentiable problems. Second, DEA makes few or no assumptions regarding the problem being optimized and searches very large spaces of candidate solution. Furthermore, unlike conventional optimization tools, it works with a population of solutions (solution vector). Since multiple strings are being processed and updated, it is likely that DEA will yield the global optima.

Differential evolution algorithm utilizes n_P d-dimensional parameter vectors $x_{i,G} = 1, 2, \ldots, n_P$ as a population for each generation G. The initial vector population is considered to be uniformly distributed over the entire parameter space. DEA generates new parameter vectors by adding the weighted difference between the two population vectors to a third vector. This operation is known as *mutation*. In the next step, the trial vector is obtained by mixing the parameter vectors obtained after mutation with the target vector. This step is known as *crossover*. If the objective function obtained corresponding to the trial vector is smaller compared to the target vector, trial vector replaces the target vector. This step is known as *selection*. Note that each population vector must serve once as the target vector in order to increase the competitions. Next, different steps of DEA have been described.

3.1.1 Mutation. A mutated vector is generated for each target vector as

$$v_{i,G+1} = x_{k_1,G} + f \cdot (x_{k_2,G} - x_{k_3,G}) \tag{5}$$

where $k_1, k_2, k_3 \in \{1, 2, \ldots, n_p\}$ are random integers that are mutually different. It is further ensured that k_1, k_2, k_3 are different from the running integer i. F is a real constant that controls the amplification of the differential variation $(x_{k_2,G} - x_{k_3,G})$. For further details, readers are referred to Refs. [63–66].

3.1.2 Crossover. The primary aim of this step is to increase the diversity of the perturbed parameter vectors. The trial vector $u_{i,G+1} = (u_{1i,G+1}, u_{2i,G+1}, \ldots, u_{di,G+1})$ is formed, where

$$u_{ji,G+1} = \begin{cases} v_{ji,G+1} & \text{if } \text{rand}(j) \le c_R \text{ or } j = \text{randi}(i) \\ x_{ji,G} & \text{if } \text{rand}(j) > c_R \text{ and } j \ne \text{randi}(i) \end{cases} \quad j = 1, 2, \ldots, d \tag{6}$$

In Eq. (6), rand(j) is the jth uniform random number and randi(i) is the randomly chosen index. c_R is the crossover parameter and resides in $[0, 1]$. For further details, readers may refer [63–66].

3.1.3 Selection. The final step of DEA is the selection. This step decides the suitability of trial vector. In this step, the trial vector $u_{i,G+1}$ is compared to the target vector $x_{i,G}$. If the value of objective function corresponding to $u_{i,G+1}$ is lower compared to that obtained using $x_{i,G}$, then $x_{i,G+1}$ is set to be $u_{i,G+1}$. On the contrary, if the value of objective function corresponding to $u_{i,G+1}$ is greater compared to that obtained using $x_{i,G}$, the old value of $x_{i,G}$ is retained.

One problem associated with any optimization algorithm is the repeated evaluation of objective and constraint functions. However, for almost all real-life problems, the objective and constraint functions are not explicitly known. In fact, expensive finite-element analysis is required for evaluating the objective and constraint functions. Furthermore, for RDO, the number of function evaluation is even more (for quantifying uncertainties).

In order to bypass this issue, a proposed approach utilizes PCFE. In Sec. 3.2, a brief description of PCFE has been provided.

3.2 Polynominal Correlated Function Expansion. PCFE [54,58,59,74], also known as generalized HDMR [62], is a general set of quantitative model assessment and analysis tool for capturing the high-dimensional relationship between sets of input and output model variables. It can be viewed as an extension of classical functional analysis of variance decomposition [75–77], where component functions are represented by utilizing the extended bases [59,62]. The unknown coefficients associated with the bases are determined by employing a homotopy algorithm (HA) [74,78,79]. HA determines the unknown coefficients by minimizing the least squared error and an objective function. The objective function defines an additional criterion that is enforced on the solution. In PCFE, the hierarchical orthogonality of the component functions is considered to be an additional criterion.

Let, $\mathbf{x} = \{x_1, x_2, \ldots . x_N\}$ be a N-dimensional vector, representing the input variables of a structural system. It is quite logical to express the output $g(\mathbf{x})$ as a finite series [77]

$$\begin{aligned} g(\mathbf{x}) &= g_0 + \sum_{k=1}^{N} \sum_{i_1 < i_2 \cdots < i_k} g_{i_1 i_2 \ldots i_N}(x_{i_1}, x_{i_2}, \ldots x_{i_N}) \\ &= g_0 + \sum_{i_1=1}^{N} g_i(x_i) + \sum_{1 \le i_1 < i_2 \le N} g_{ij}(x_i, x_j) \\ &\quad + \cdots + g_{12\ldots N}(x_1, x_2, \ldots, x_N) \end{aligned} \tag{7}$$

where g_0 is a constant and represents the mean response. The terms in Eq. (7) reflecting the independent effects only are termed as first-order component function and denoted as $g_{i_1}(x_{i_1})$. Similarly, the terms reflecting the bivariate effects are termed as second-order component function and denoted by $g_{i_1 i_2}(x_{i_1}, x_{i_2})$. The constant g_0 is termed as zeroth-order component function.

Assume two subspace R and B in Hilbert space are spanned by basis $\{r_1, r_2, \ldots, r_l\}$ and $\{b_1, b_2, \ldots, b_m\}$, respectively. Now if (i) $B \supset R$ and (ii) $B = R + R^{\perp}$, where $R^{\perp}$ is the orthogonal complement subspace of R in B, B is termed as extended basis, and R is termed as nonextended basis [59,62].

Now if ψ be some suitable basis for $\mathbf{x} \subseteq \mathbf{X}$, where $\mathbf{X} := \{1, 2, \ldots, N\}$, Eq. (7) can be rewritten as [59,62]

$$g(\mathbf{x}) = g_0 + \sum_{k=1}^{N} \left\{ \sum_{i_1=1}^{N-k+1} \cdots \sum_{i_k=i_{k-1}}^{N} \sum_{r=1}^{k} \left[\sum_{m_1=1}^{\infty} \sum_{m_2=1}^{\infty} \cdots \sum_{m_r=1}^{\infty} \alpha_{m_1 m_2 \ldots m_r}^{(i_1 i_2 \ldots i_k) i_r} \psi_{m_1}^{i_1} \ldots \psi_{m_r}^{i_r} \right] \right\} \tag{8}$$

Noting that most real-life problems exhibit only lower-order cooperative effect, the higher-order component functions can be truncated. Considering up to Mth order component function and sth order basis yields

$$\hat{g}(\mathbf{x}) = g_0 + \sum_{k=1}^{M} \left\{ \sum_{i_1=1}^{N-k+1} \cdots \sum_{i_k=i_{k-1}}^{N} \sum_{r=1}^{k} \left[\sum_{m_1=1}^{s} \sum_{m_2=1}^{s} \cdots \sum_{m_r=1}^{s} \alpha_{m_1 m_2 \ldots m_r}^{(i_1 i_2 \ldots i_k) i_r} \psi_{m_1}^{i_1} \ldots \psi_{m_r}^{i_r} \right] \right\} \tag{9}$$

Once the unknown coefficients associated with the bases are determined, Eq. (9) represents the basic functional form of PCFE.

Remark 1. As already established in previous studies [54, 55,59], most of the real-life problems only involve a lower-order co-operative effect. In fact, results obtained using second-order ($M = 2$) PCFE is accurate for real-life problems [54,55,59]. Based on this observation, a second-order PCFE has been utilized in this work.

An essential condition associated with Eq. (9) is the hierarchical orthogonality of the component functions [59,62], which requires a higher-order component function to be orthogonal with all the lower-order component functions. To determine the unknown coefficients $\boldsymbol{\alpha}$ while satisfying the orthogonality criteria, an HA [55,79] is employed. This algorithm treats the orthogonality of component functions as an additional condition and determines the unknown coefficients by minimizing the least-squared error.

Rewriting Eq. (9) in matrix form

$$\boldsymbol{\Psi}\boldsymbol{\alpha} = \mathbf{d} \tag{10}$$

where $\boldsymbol{\Psi}$ and $\boldsymbol{\alpha}$ consists of the basis functions and unknown coefficients, respectively. If $\mathbf{g} = \{g_1, g_2, \ldots, g_p\}^{\mathrm{T}}$ be the observed responses at q sets of sample points, then

$$\mathbf{d} = \mathbf{g} - \bar{\mathbf{g}} \tag{11}$$

where $\bar{\mathbf{g}} = \{g_0, g_0, \ldots, g_0\}^{\mathrm{T}}$. Premultiplying Eq. (11) by $\boldsymbol{\Psi}^{\mathrm{T}}$, one obtains

$$\mathbf{B}\boldsymbol{\alpha} = \mathbf{C} \tag{12}$$

where $\mathbf{B} = \boldsymbol{\Psi}^{\mathrm{T}}\boldsymbol{\Psi}$ and $\mathbf{C} = \boldsymbol{\Psi}^{\mathrm{T}}\mathbf{d}$. From Eq. (9), it is evident that as long as $N > 1$, $\boldsymbol{\Psi}$ have identical columns. Thus, $\mathbf{B}$ is having identical rows which can be treated as redundants. Removing the redundants

$$\mathbf{B}'\boldsymbol{\alpha} = \mathbf{C}' \tag{13}$$

where $\mathbf{B}'$ and $\mathbf{C}'$ are, respectively, $\mathbf{B}$ and $\mathbf{C}$ after removing the redundants. Equation (13) represents a set of underdetermined

system. All the solutions of Eq. (13) can be represented into a generalized form as

$$\begin{aligned}\boldsymbol{\alpha} &= (\mathbf{B}')^{-1}\mathbf{C}' + (\mathbf{I} - (\mathbf{B}')^{-1}\mathbf{B}')v(s) \\ &= (\mathbf{B}')^{-1}\mathbf{C}' + \mathbf{P}v(s)\end{aligned} \tag{14}$$

where $(\mathbf{B}')^{-1}$ denotes the generalized inverse of $\mathbf{B}'$ satisfying part or all four Penrose condition [80]. $\mathbf{I}$ represents an identity matrix of dimension $q \times q$. All the solution of $\boldsymbol{\alpha}$ obtained from Eq. (14) compose a completely connected submanifold $\mathcal{M} \subset \Re^q$. In HA, one seeks the solution that minimizes the least squared error and satisfies the orthogonality criteria defined in Refs. [59,62].

Employing HA [55,79], the unknown coefficient vector $\boldsymbol{\alpha}$ is obtained as [59,62]

$$\boldsymbol{\alpha}_{\mathrm{HA}} = [\mathbf{V}_{q-r}(\mathbf{U}_{q-r}^{\mathrm{T}}\mathbf{V}_{q-r})^{-1}\mathbf{U}_{q-r}^{\mathrm{T}}]\boldsymbol{\alpha}_0 \tag{15}$$

where $\mathbf{U}$ and $\mathbf{V}$ are matrices obtained by singular value decomposition of $\mathbf{PW}$ matrix, where $\mathbf{W}$ is the weight matrix obtained by imposing the orthogonality condition. $\boldsymbol{\alpha}_0$ is the solution obtained using least squared minimization. Equation (15) is the practical formula obtained using homotopy algorithm. For a detailed description of the homotopy algorithm, interested readers may refer [55,79]. For details regarding formulation of the orthogonality criteria and weight matrix, that are used as additional criteria, interested readers are referred to Refs. [54,59,62,74].

A pseudo-code for determining unknown coefficients of PCFE is shown in Algorithm 1.

3.3 Proposed Approach. In this section, a coupled framework for RDO has been presented. The framework proposed has been developed by coupling PCFE into the framework of DEA. However, before coupling PCFE into DEA, it is essential to determine the optimum basis order. The steps involved for determining the optimum basis order are described below.

Step 1: Provide the tolerance limit ϵ_1 and ϵ_2.
Step 2: Set PCFE order $M = 2$ and basis order $s = 1$. Input initial sample size. Set $counter = 1$.
Step 3: Generate sample points
Step 4: Formulate PCFE-based operational model using Algorithm 1.
Step 5: **If** $counter = 1$, compute the variance of the unknown coefficients ($\sigma_\alpha^{\mathrm{counter}}$). Generate additional sample points. **Else** compute the change in variance of the unknown coefficients $\Delta\sigma_\alpha^{\mathrm{counter}} = \sigma_\alpha^{\mathrm{counter}} - \sigma_\alpha^{\mathrm{counter}-1}$. If $\Delta\sigma_\alpha^{\mathrm{counter}} > \epsilon_1$, generate additional sample points, set counter = counter + 1 and **go to** Step 4. Else **go to** Step 6.
Step 6: Compute error ($e\hat{\mathrm{n}}_1$) of the generated PCFE-based operational model using leave-one-out statistical test. If $e\hat{\mathrm{n}}_1 > \epsilon 2$, set $s = s + 1$ and **go to** Step 3. Else **stop**.

Once the optimum basis order is determined, explicit expressions for the objective and/or constraint functions are generated using the PCFE-based operational model. After that, DEA is utilized to solve the RDO problem formulated by using the PCFE-based objective and constraint functions. A flow chart for performing RDO using DEA–PCFE is shown in Fig. 2.

DEA–PCFE has several unique properties:

- The number of actual function evaluation using DEA–PCFE is significantly less as compared to other popular techniques available in the literature. This is because the terms in PCFE are arranged based on the degree of cooperativity between a finite numbers of random variables, and the lower-order component function of PCFE inherently incorporates the higher-order nonlinearity. As a result, if the response is highly nonlinear and higher dimensional cooperative effects of multiple random variables are rapidly diminishing, PCFE is highly effective. In this context, it may be noted that most of the real-life problems generally involve lower-order cooperative effect [81]. Furthermore, the elite convergence rate of DEA makes DEA–PCFE an ideal tool for RDO.
- PCFE is a finite series consisting of 2^N component functions, where N is the number of random variables. Thus, if the component functions are convergent, PCFE provides an exact solution.
- PCFE is a mean-square convergent series because it minimizes the mean square error from truncation after a finite number of cooperative terms.

Algorithm 1 Pseudo-code for PCFE

1. Initialize: Provide order of PCFE, input variable (var) type and corresponding parameters. Identify variable bounds based on the input parameters. Generate sample points (N_s) within the bounds and obtain response ($g(x)$) by actual finite element model analysis.
2. $(\mathrm{var})_i^j \leftarrow \dfrac{(\mathrm{var})_i^j - \min(\mathrm{var})_i}{\max(\mathrm{var})_i - \min(\mathrm{var})_i} \forall i, j$
3. $g_0 \leftarrow \dfrac{1}{N_s}\sum_s g(x_s)$
4. **for** $i = 1 : N_s$
   $d_i \leftarrow g(x_i) - g_0$
   end for
5. $\boldsymbol{\Psi} \leftarrow [\,\psi(\mathbf{x}^1) \quad \psi(\mathbf{x}^2) \quad \cdots \quad \psi(\mathbf{x}^{N_s})\,]^{\mathrm{T}}$ where

$$\psi(\mathbf{x}^r)^{\mathrm{T}} \leftarrow [\,\psi_1^1(x_1^r) \quad \psi_2^1(x_1^r) \quad \cdots \quad \psi_k^1(x_1^r) \quad \psi_1^2(x_2^r) \quad \cdots \quad \psi_1^1(x_1^r) \quad \cdots \quad \psi_m^{N-2}(x_{N-2}^r)\psi_m^{N-1}(x_{N-1}^r) \quad \psi_m^{N-1}(x_{N-1}^r)\psi_m^N(x_N^r)$$

6. $\mathbf{d} \leftarrow [\,d_1 \quad d_2 \quad \cdots \quad d_{N_s}\,]^{\mathrm{T}}$
7. $\mathbf{B} \leftarrow \boldsymbol{\Psi}^{\mathrm{T}}\boldsymbol{\Psi}$ and $\mathbf{C} \leftarrow \boldsymbol{\Psi}^{\mathrm{T}}\mathbf{d}$
8. $[\mathbf{B}' \quad \mathbf{d}'] \leftarrow \mathrm{remove\_redundants}(\mathbf{B}, \mathbf{d})$
9. $\mathbf{P} \leftarrow \mathbf{I} - (\mathbf{B}')^{-1}\mathbf{B}'$
10. $\mathbf{W} \leftarrow \mathrm{form\_weight}(\boldsymbol{\Psi})$
11. $[\mathbf{U} \quad \mathbf{V}] \leftarrow svd(\mathbf{PW})$
12. $\boldsymbol{\alpha}_{\mathrm{HA}} \leftarrow [\mathbf{V}_{q-r}(\mathbf{U}_{q-r}^{\mathrm{T}}\mathbf{V}_{q-r})^{-1}\mathbf{U}_{q-r}^{\mathrm{T}}]\boldsymbol{\alpha}_0$

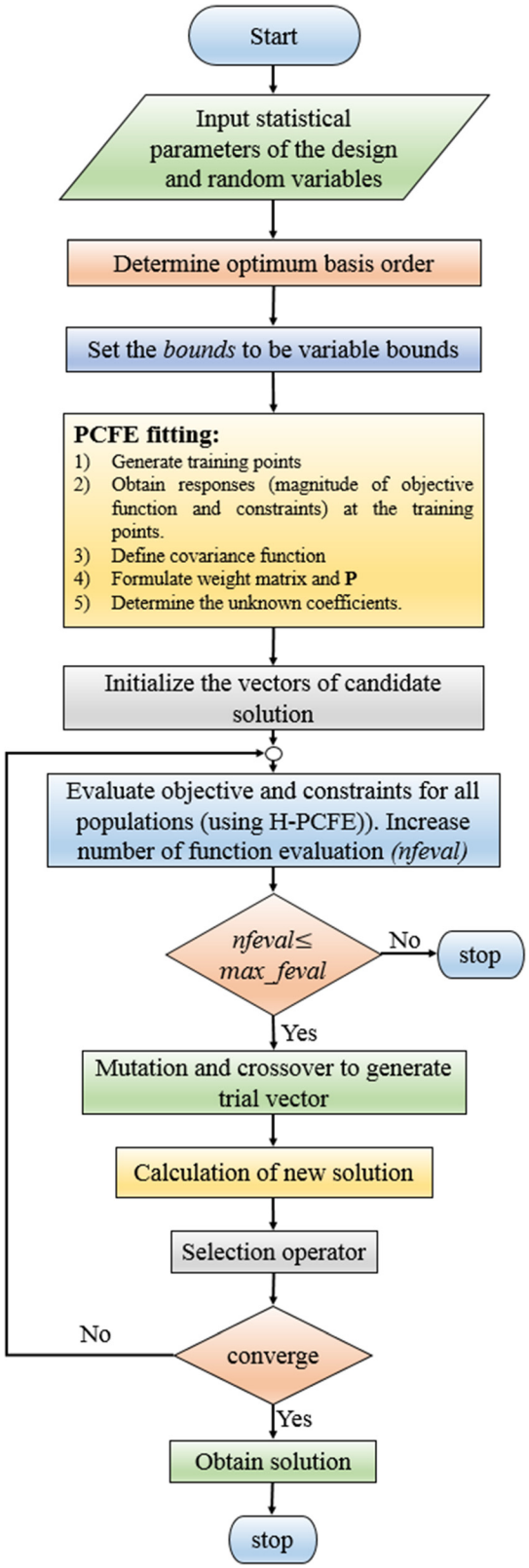

Fig. 2 Flowchart for DEA–PCFE

- The proposed approach utilizes PCFE, which is optimum in Fourier sense. This is due to the fact that the unknown coefficients associated with the basis are determined by considering the hierarchical orthogonality of the component functions.

The above features classify DEA–PCFE as an ideal tool for RDO.

4 Validation

In this section, DEA–PCFE has been validated against popular approaches available in the literature. To be specific, two benchmark problems have been solved using the proposed approach. For both the problems, the population size and the generation size in DEA are considered to be 50 and 100, respectively. The crossover parameter and the mutation parameter are set to be 0.5 and 0.8, respectively. Second-order PCFE model has been utilized in this study. For all the problems, the optimum order of basis is determined by using the proposed iterative algorithm. The sample points required to formulate the PCFE model are generated by using a Sobol sequence. However, it is worth mentioning that the proposed DEA–PCFE is applicable to both uniformly and nonuniformly distributed sample points.

4.1 A Mathematical Function. In the first problem, RDO of a mathematical function has been performed. This problem is a well-known benchmark problem for RDO techniques and has been previously solved by Refs. [8,82] The optimization problem reads

$$\begin{aligned} &\min_{d\in D} \quad c_O(\mathbf{d}) = \frac{\sigma_{\mathbf{d}}\left(y_0(\mathbf{X})\right)}{15} \\ &\text{s.t. } c_k(\mathbf{d}) = 3\sigma_{\mathbf{d}}\left(y_1(\mathbf{X})\right) - \langle y_1(\mathbf{X})\rangle \\ &1 < d_1, d_2 < 10 \end{aligned} \tag{16}$$

where the two functions $y_0(\mathbf{X})$ and $y_1(\mathbf{X})$ are given as

$$y_0(\mathbf{X}) = (X_1 - 4)^3 + (X_1 - 3)^4 + (X_2 - 5)^2 + 10 \tag{17}$$

and

$$y_1(\mathbf{X}) = X_1 + X_2 - 6.45 \tag{18}$$

Both the design variables follow Gaussian distribution with a standard deviation of 0.4.

Differential evolution algorithm–polynominal correlated function expansion has been utilized to solve this problem. Table 1 shows the optimum design obtained using the proposed approach. Results obtained have been compared with tensor product quadrature (TPQ), Taylor's series (TS), Gaussian process (GP), polynomial chaos expansion (PCE) [36], and sparse grid collocation technique (SGC) [83]. It is observed that DEA–PCFE yields the best results as compared to the other techniques for RDO. Furthermore, the total number of function evaluation using DEA–PCFE ($n_t = 76$) is significantly less as compared to TPQ ($n_t = 162$), TS ($n_t = 90$), GP ($n_t = 256$), third order PCE ($n_t = 160$), and SGC (level five) ($n_t = 795$).

4.2 2-Bar Truss. In this example, a 2-bar truss element, as shown in Fig. 3, has been considered [8,82]. The system is having five independent random variables, namely cross-sectional area X_1, the horizontal span (half) X_2, material density X_3, load X_4, and tensile strength X_5. The details of random variables are provided in Table 2. The design variables are $d_1 = E(X_1)$ and $d_2 = E(X_2)$. The objective of this problem is to minimize the second moment properties of mass of the structure, given that limiting stresses in both members are below the material yield stress. Consequently, the RDO problem is formulated as

Table 1 Optimized parameters for first validation problem

Methods	d_1	d_2	$c_O(\mathbf{d}^a)$	N_s[a]
TPQ[b]	3.45	5.00	0.086	162
TS[b]	3.50	4.99	0.090	90
GP	3.37	5.00	0.076	256
PCE	3.33	4.99	0.076	160
SGC	3.36	5.00	0.076	795
DEA–PCFE	3.35	4.99	0.076	76

[a]No. of actual simulations.
[b]Obtained from Ref. [8].

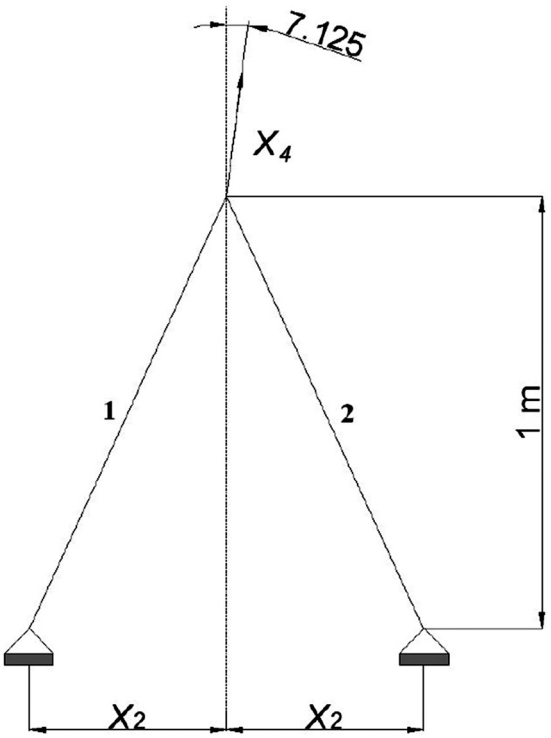

Fig. 3 2-bar truss structure considered for validation

Table 2 Properties of random variables

Variable	Mean	COV	Type
X_1	d_1	0.02	Gaussian
X_2	d_2	0.02	Gaussian
X_3	10,000	0.2	Beta[a]
X_4	800	0.25	Gumbel
X_5	1050	0.24	lognormal

[a]For beta distribution, both parameters are five.

Table 3 Robust design of 2-bar truss

Methods	d_1	d_2	$c_O(\mathbf{d}^a)$	N_s[a]
TPQ[b]	11.567	0.3767	1.239	7722
TS[b]	10.957	0.3770	1.174	648
GP	12.783	0.3770	1.37	1280
PCE	12.6268	1.0149	1.80	1536
SGC	11.3302	0.3771	1.21	42,075
DEA-PCFE	10.957	0.3770	1.174	640

[a]No. of actual simulations.
[b]Obtained from Ref. [8].

$$\begin{aligned} \min_{d\in D} \quad & c_O(\mathbf{d}) = \beta_1 \frac{E\big(y_0(\mathbf{X})\big)}{10} + (1-\beta_1)\frac{\sigma\big(y_0(\mathbf{X})\big)}{2} \\ \text{s.t.} \quad & c_1(\mathbf{d}) = 3\sigma\big(y_1(\mathbf{X})\big) - E\big(y_1(\mathbf{X})\big) \le 0 \\ & c_2(\mathbf{d}) = 3\sigma\big(y_2(\mathbf{X})\big) - E\big(y_2(\mathbf{X})\big) \le 0 \\ & 0.2\,\text{cm}^2 \le d_1 \le 20\,\text{cm}^2,\ 0.1\ \text{m} \le d_2 \le 1.6\ \text{m} \end{aligned} \tag{19}$$

where y_0, y_1, and y_2 are, respectively, mass of the structure, stress in member 1, and stress in member 2.

Table 3 shows the RDO results obtained using DEA–PCFE, TPQ, TS, GP, PCE [36], and SGC [83]. It is observed that DEA–PCFE ($c_O(\mathbf{d}^*) = 1.189$, $N_s = 640$) outperforms TPQ ($c_O(\mathbf{d}^*) = 1.239$, $N_s = 7722$), GP ($c_O(\mathbf{d}^*) = 1.37$, $N_s = 1280$), PCE ($c_O(\mathbf{d}^*) = 1.80$, $N_s = 1536$), and SGC ($c_O(\mathbf{d}^*) = 1.21$, $N_s = 42{,}075$) both in terms of accuracy and efficiency. DEA–PCFE and TS yield the best results ($c_O(\mathbf{d}^*) = 1.174$). However, the number of function evaluations using DEA–PCFE ($N_s = 640$) is less, as compared to TS ($N_s = 648$).

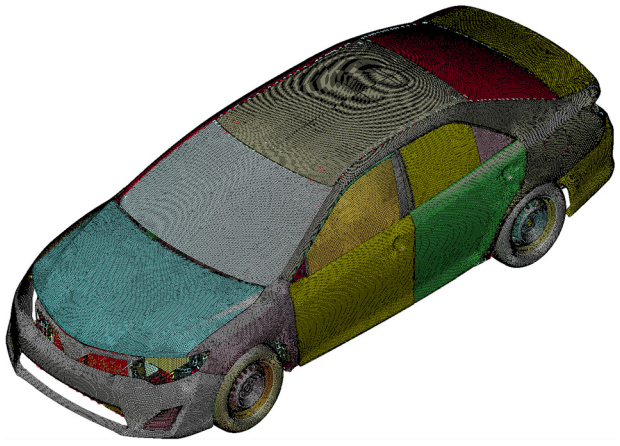

Fig. 4 Vehicle model for side impact problem

Table 4 Safety criteria as per European Enhanced Vehicle-Safety Committee

Performance		Top safety rating criteria
Abdomen load		≤ 1
Rib deflection	Upper Middle Lower	≤ 22
VC (m/s)	Upper Middle Lower	≤ 0.32
Pubic symphysis force (kN)		≤ 3
HIC		≤ 650

5 Crashworthiness of Vehicle Due to Side Impact

In this section, the detailed problem formulation including the FE model of vehicle and safety regulations has been presented. The problem description for RDO and the results obtained have been presented toward the end of this section.

5.1 Vehicle Model Description. The proposed approach is utilized for RDO of a large-scale vehicle as shown in Fig. 4. RDO of the vehicle against crashworthiness due to side impact has been investigated. The system model includes a full-vehicle FE structure model[1] a side impact dummy FE model and a side barrier [9,84]. The vehicle model consists of 1.7M nodes. In the FE simulation, the initial velocity of the barrier is considered to be 49.89 kmph. RBDO of the above-mentioned vehicle is already been carried out by Ref. [9]. In this study, the primary objective is to perform RDO of the vehicle using the proposed approach.

5.2 Safety Regulations. It is essential for the vehicle design to satisfy the internal and regulated side impact requirements. Two primary side impact protection guidelines that are quite popular in the vehicle market are the (i) National Highway Traffic Safety Administration (NHTSA) side impact procedures for the Federal Motor Vehicle Safety Standard (FMVSS) and Canadian Motor Vehicle Safety Standard (CMVSS) and (ii) European Enhanced Vehicle-Safety Committee (EEVC) side impact

[1]Obtained from http://www.ncac.gwu.edu/archives/model/index.html

Table 5 Statistical parameters of random parameters in Eq. (20)

Random variables	Std. dev.	Type	$\mathbf{d}^L$	$\mathbf{d}_i$	$\mathbf{d}^U$
B-pillar inner (mm)	0.100	Normal	0.500	1.000	1.500
B-pillar reinforce (mm)	0.100	Normal	0.450	1.000	1.350
Floor side inner (mm)	0.100	Normal	0.500	1.000	1.500
Cross member	0.100	Normal	0.500	1.000	1.500
Door beam (mm)	0.100	Normal	0.875	2.000	2.625
Door belt line (mm)	0.100	Normal	0.400	1.000	1.200
Roof rail (mm)	0.100	Normal	0.400	1.000	1.200
Mat. B-pillar inner (GPa)	0.006	Normal	0.192	0.300	0.345
Mat. floor side inner (GPa)	0.006	Normal	0.192	0.300	0.345
Barrier height (mm)	10	Normal	Not design variable		
Barrier hitting (mm)	10	Normal	Not design variable		

Table 6 Comparison of RDO results obtained using various methods

	Optimum design							
	Mass (mean)				Lower rib deflection (variance)			
β	PCE	SGC	DEA–PCFE	FE	PCE	SGC	DEA–PCFE	FE
0	30.50	30.44	30.69	30.69	1.19	1.19	1.18	1.18
0.1	29.12	28.89	29.11	29.11	1.183	1.19	1.182	1.182
0.4	26.51	27.02	26.66	26.66	1.22	1.212	1.217	1.217
0.5	26.07	26.00	26.02	26.02	1.227	1.223	1.223	1.223

DEA–PCFE requires 256 actual FE simulations.
PCE requires 2048 actual FE simulations.
SGC requires 5300 actual function evaluations.

Table 7 Design variables at optimum point obtained using DEA–PCFE

	$\beta = 0$				$\beta = 0.1$				$\beta = 0.4$				$\beta = 0.5$			
Variables	PCE	SGC	DEA–PCFE	FE	PCE	SGC	DEA–PCFE	FE	PCE	SGC	DEA–PCFE	FE	PCE	SGC	DEA–PCFE	FE
d_1	1.50	1.50	1.50	1.50	1.50	1.50	1.50	1.50	0.95	1.09	0.99	0.99	0.87	0.86	0.87	0.86
d_2	0.69	0.70	0.72	0.71	0.72	0.73	0.72	0.72	0.67	0.68	0.67	0.67	0.67	0.67	0.67	0.67
d_3	0.50	0.50	0.50	0.50	0.50	0.50	0.50	0.50	0.50	0.50	0.50	0.50	0.50	0.50	0.50	0.50
d_4	1.27	1.25	1.32	1.31	0.88	0.81	0.87	0.87	1.15	1.09	1.16	1.15	1.15	1.16	1.16	1.16
d_5	2.63	2.62	2.63	2.63	2.62	2.63	2.63	2.62	2.27	2.25	2.19	2.21	2.24	2.18	2.19	2.19
d_6	0.68	0.70	0.62	0.62	0.65	0.63	0.66	0.65	0.62	0.65	0.64	0.64	0.63	0.64	0.64	0.64
d_7	1.20	1.20	1.20	1.20	1.20	1.20	1.20	1.20	1.20	1.20	1.20	1.20	1.20	1.20	1.20	1.20
d_8	0.22	0.22	0.22	0.22	0.22	0.21	0.22	0.22	0.33	0.31	0.35	0.32	0.34	0.35	0.35	0.35
d_9	0.28	0.29	0.29	0.29	0.34	0.34	0.35	0.35	0.19	0.22	0.19	0.20	0.19	0.19	0.19	0.19

procedure for European vehicle. In this study, EEVC side impact criteria, as shown in Table 4 [9,84], has been considered.

5.3 Robust Crashworthiness Design Optimization for Side Impact. The RDO problem for crashworthiness of vehicle due to side impact is formulated as

$$\begin{aligned}
&\text{minimize } \beta\frac{W}{W_0}+(1-\beta)\frac{\sigma_H}{\sigma_{H_0}}\\
&\text{subject to } \mu_{\text{AL}}+k.\sigma_{\text{AL}}\le 1\,\text{kN}\\
&\quad \mu_{(\text{U/M/L})\text{VC}}+k.\sigma_{(\text{U/M/L})\text{VC}}\le 0.32\,\text{m/s}\\
&\quad \mu_{(\text{U/M/L})\text{deflection}}+k.\sigma_{(\text{U/M/L})\text{deflection}}\le 32\,\text{mm}\\
&\quad \mu_{\text{PSF}}+k.\sigma_{\text{PSF}}\le 4\,\text{kN}\\
&\quad \mu_{V_{\text{B-PILLAR}}}+k.\sigma_{V_{\text{B-PILLAR}}}\le 9.9\,\text{mm/ms}\\
&\quad \mu_{V_{\text{FD}}}+k.\sigma_{V_{\text{FD}}}\le 15.7\,\text{mm/ms}\\
&\quad \mathbf{d}^L\le\mathbf{d}\le\mathbf{d}^{\mathbf{U}},\ \mathbf{d}\in\mathbb{R}^9,\ \mathbf{X}\in\mathbb{R}^{11}
\end{aligned} \tag{20}$$

where W is the mass of the vehicle and H is the lower rib deflection. PSF, B − PILLAR and V_{FD}, respectively, denote pubic symphysis force (PSF), velocity of B-pillar at midpoint and velocity of front door at B-pillar. k in Eq. (20) denotes the sigma level. Based on users' requirement, its value is to be chosen appropriately. μ and σ denote mean and standard deviation, respectively. The system is having eleven random variables, which include thickness $(d_1 - d_7)$, material properties of critical part (d_8, d_9), barrier height, and hitting position. Only the first nine random parameters are considered to be design variables. Barrier height and hitting position may vary from −30 mm to 30 mm [9]. All the random variables are assumed to be normally distributed. Details of the random variables are given in Table 5.

5.4 Results and Discussion. Using the information provided in the Secs. 5.1–5.3, RDO for crashworthiness of vehicle due to side impact has been carried out. From practical point of view, $k = 3$ in Eq. (20) has been considered. The training points required for PCFE and PCE has been generated using a Sobol's sampling scheme [85,86].

Tables 6 and 7 show the result obtained using the various methods. The benchmark solution has been obtained by actual finite-element simulation. The results have been calculated corresponding to $\beta = [0, 0.1, 0.4, 0.5]$. As expected, with an increase in β, the mass (mean) decreases and low rib deflection (variance) increases. For all the cases, results obtained using the proposed DEA–PCFE are in excellent agreement with the benchmark solution. The other approaches, namely PCE and SGC, also yield satisfactory results. However, the number of actual FE simulation required using the proposed approach ($N_s = 256$) is significantly less as compared to PCE ($N_s = 2048$) and SGC ($N_s = 5300$).

6 Conclusion

A novel approach, referred to as DEA based on PCFE, is presented for robust design optimization of vehicle crashworthiness subjected to side impact. DEA–PCFE is formulated by coupling PCFE with DEA. While PCFE is utilized to generate an approximate surrogate model for the uncertain objective functions and/or constraints, DEA is utilized to perform the optimization. The order of basis involved in PCFE is determined by employing an adaptive scheme. The proposed approach reduces the actual function evaluation significantly and is thus suitable for large-scale problems. DEA–PCFE has been validated against popular methods available in literature.

A full-scale finite element model[2], has been optimized. The problem considered is having nine design variables and eleven random variables. Various case studies by providing various emphases on the mean and deviation components have also been performed. For all the cases, results obtained using DEA–PCFE are in excellent agreement with FE simulations. Furthermore, DEA–PCFE is highly efficient as compared to available techniques.

[2]Obtained from http://www.ncac.gwu.edu/archives/model/index.html

Acknowledgment

SC and RC acknowledge the support of CSIR via grant no. 22(0712)/16/EMR-II. TC acknowledges the support of MHRD, Government of India.

Nomenclature

$\mathbf{d}$ = design variables in vehicle crashworthiness optimization
g_0 = zeroth-order component function of PCFE
$g(\mathbf{x})$ = output
$\hat{g}(\mathbf{x})$ = approximated output
H = low rib deflection
k = sigma level
n_p = population size in DEA
rand(j) = jth uniform random number
randi = randomly chosen integer
$u_{i,G+1}U$ = trial vector
V_{FD} = velocity of front door
$v(s)$ = free function vector
$\mathbf{W}$ = weight matrix
W = mass of vehicle
$\mathbf{x}$ = input vector
$x_{i,G}$ = parameter vector in generation G
x_L = lower limit of x
x_U = upper limit of x
α = unknown coefficient
α_{HA} = solution obtained using homotopy algorithm
β = weighing factor in RDO objective function
$\mu(\bullet)$ = mean
μ^*, σ^* = ideal designs
$\sigma(\bullet)$ = standard deviation
ψ = basis function

References

[1] Kurtaran, H., Eskandarian, A., Marzougui, D., and Bedewi, N. E., 2002, "Crashworthiness Design Optimization Using Successive Response Surface Approximations," Comput. Mech., **29**(4–5), pp. 409–421.
[2] Avalle, M., Chiandussi, G., and Belingardi, G., 2002, "Design Optimization by Response Surface Methodology: Application to Crashworthiness Design of Vehicle Structures," Struct. Multidiscip. Optim., **24**(4), pp. 325–332.
[3] Duddeck, F., 2007, "Multidisciplinary Optimization of Car Bodies," Struct. Multidiscip. Optim., **35**(4), pp. 375–389.
[4] Fang, H., Rais-Rohani, M., Liu, Z., and Horstemeyer, M., 2005, "A Comparative Study of Metamodeling Methods for Multiobjective Crashworthiness Optimization," Comput. Struct., **83**(25–26), pp. 2121–2136.
[5] Forsberg, J., and Nilsson, L., 2006, "Evaluation of Response Surface Methodologies Used in Crashworthiness Optimization," Int. J. Impact Eng., **32**(5), pp. 759–777.
[6] Gu, L., Yang, R., Tho, C., Makowskit, M., Faruquet, O., and Li, Y., 2004, "Optimisation and Robustness for Crashworthiness of Side Impact," Int. J. Veh. Des., **26**(4), pp. 348–360.
[7] Hou, S., Li, Q., Long, S., Yang, X., and Li, W., 2008, "Multiobjective Optimization of Multi-Cell Sections for the Crashworthiness Design," Int. J. Impact Eng., **35**(11), pp. 1355–1367.
[8] Lee, S. H., Chen, W., and Kwak, B. M., 2008, "Robust Design With Arbitrary Distributions Using Gauss-Type Quadrature Formula," Struct. Multidiscip. Optim., **39**(3), pp. 227–243.
[9] Youn, B., Choi, K., Yang, R.-J., and Gu, L., 2004, "Reliability-Based Design Optimization for Crashworthiness of Vehicle Side Impact," Struct. Multidiscip. Optim., **26**(3–4), pp. 272–283.
[10] Chen, X., Park, E. J., and Xiu, D., 2013, "A Flexible Numerical Approach for Quantification of Epistemic Uncertainty," J. Comput. Phys., **240**, pp. 211–224.
[11] Jakeman, J., Eldred, M., and Xiu, D., 2010, "Numerical Approach for Quantification of Epistemic Uncertainty," J. Comput. Phys., **229**(12), pp. 4648–4663.
[12] Der Kiureghian, A., and Ditlevsen, O., 2009, "Aleatory or Epistemic? Does It Matter?" Struct. Saf., **31**(2), pp. 105–112.
[13] Ross, J. L., Ozbek, M. M., and Pinder, G. F., 2009, "Aleatoric and Epistemic Uncertainty in Groundwater Flow and Transport Simulation," Water Resour. Res., **45**(12), p. W00b15.
[14] Huang, B., and Du, X., 2007, "Analytical Robustness Assessment for Robust Design," Struct. Multidiscip. Optim., **34**(2), pp. 123–137.
[15] Zang, C., Friswell, M. I., and Mottershead, J. E., 2005, "A Review of Robust Optimal Design and Its Application in Dynamics," Comput. Struct., **83**(4–5), pp. 315–326.
[16] Youn, B. D., and Xi, Z., 2008, "Reliability-Based Robust Design Optimization Using the Eigenvector Dimension Reduction (EDR) Method," Struct. Multidiscip. Optim., **37**(5), pp. 475–492.
[17] Dubourg, V., Sudret, B., and Bourinet, M., 2011, "Reliability-Based Design Optimization Using Kriging Surrogates and Subset Simulation," Struct. Multidiscip. Optim., **44**(5), pp. 673–690.
[18] Dubourg, V., 2011, "Adaptive Surrogate Models for Reliability Analysis and Reliability-Based-Design-Optimization," Ph.D. thesis, Blaise Pascal University Clermont II, Clermont-Ferrand, France.
[19] Dubourg, V., Sudret, B., and Deheeger, F., 2013, "Metamodel-Based Importance Sampling for Structural Reliability Analysis," Probab. Eng. Mech., **33**, pp. 47–57.
[20] Debbarma, R., Chakraborty, S., and Ghosh, S., 2010, "Unconditional Reliability-Based Design of Tuned Liquid Column Dampers Under Stochastic Earthquake Load Considering System Parameters Uncertainties," J. Earthquake Eng., **14**(7), pp. 970–988.
[21] Marczyk, J., 2000, "Stochastic Multidisciplinary Improvement: Beyond Optimization," AIAA Paper No. 2000-4929.
[22] Yao, W., Chen, X., Luo, W., van Tooren, M., and Guo, J., 2011, "Review of Uncertainty-Based Multidisciplinary Design Optimization Methods for Aerospace Vehicles," Prog. Aerosp. Sci., **47**(6), pp. 450–479.
[23] Fang, J., Gao, Y., Sun, G., Xu, C., and Li, Q., 2015, "Multiobjective Robust Design Optimization of Fatigue Life for a Truck Cab," Reliab. Eng. Syst. Saf., **135**, pp. 1–8.
[24] Diez, M., and Peri, D., 2010, "Robust Optimization for Ship Concept Design," Ocean Eng., **37**(11–12), pp. 966–977.
[25] Roy, B. K., and Chakraborty, S., 2015, "Robust Optimum Design of Base Isolation System in Seismic Vibration Control of Structures Under Random System Parameters," Struct. Saf., **55**, pp. 49–59.
[26] Roy, B. K., Chakraborty, S., and Mihsra, S. K., 2012, "Robust Optimum Design of Base Isolation System in Seismic Vibration Control of Structures Under Uncertain Bounded System Parameters," J. Vib. Control, **20**(5), pp. 786–800.
[27] Gerstl, S., 1973, "Second-Order Perturbation-Theory and Its Application to Sensitivity Studies in Shield Design Calculations," Trans. Am. Nucl. Soc., **16**, pp. 342–343.
[28] Kamiski, M., 2004, "Stochastic Perturbation Approach to the Wavelet-Based Analysis," Numer. Linear Algebra Appl., **11**(4), pp. 355–370.
[29] Echard, B., Gayton, N., and Lemaire, M., 2011, "AK-MCS: An Active Learning Reliability Method Combining Kriging and Monte Carlo Simulation," Struct. Saf., **33**(2), pp. 145–154.
[30] Echard, B., Gayton, N., Lemaire, M., and Relun, N., 2013, "A Combined Importance Sampling and Kriging Reliability Method for Small Failure Probabilities With Time-Demanding Numerical Models," Reliab. Eng. Syst. Saf., **111**, pp. 232–240.
[31] Kaymaz, I., 2005, "Application of Kriging Method to Structural Reliability Problems," Struct. Saf., **27**(2), pp. 133–151.
[32] Ng, S. H., and Yin, J., 2013, "Bayesian Kriging Analysis and Design for Stochastic Simulations," ACM Trans. Model. Comput. Simul., **22**(3), p. 17.
[33] Zhao, W., Liu, J. K., Li, X. Y., Yang, Q. W., and Chen, Y. Y., 2013, "A Moving Kriging Interpolation Response Surface Method for Structural Reliability Analysis," Comput. Model. Eng. Sci., **93**(6), pp. 469–488.
[34] Mukhopadhyay, T., Chakraborty, S., Dey, S., Adhikari, S., and Chowdhury, R., 2016, "A Critical Assessment of Kriging Model Variants for High-Fidelity Uncertainty Quantification in Dynamics of Composite Shells," Arch. Comput. Methods Eng., (in press).
[35] Desai, A., Witteveen, J. A. S., and Sarkar, S., 2013, "Uncertainty Quantification of a Nonlinear Aeroelastic System Using Polynomial Chaos Expansion With Constant Phase Interpolation," ASME J. Vib. Acoust., **135**(5), p. 051034.
[36] Jacquelin, E., Adhikari, S., Sinou, J., and Friswell, M. I., 2014, "Polynomial Chaos Expansion and Steady-State Response of a Class of Random Dynamical Systems," J. Eng. Mech., **141**(4), pp. 1–11.
[37] Pascual, B., and Adhikari, S., 2012, "A Reduced Polynomial Chaos Expansion Method for the Stochastic Finite Element Analysis," Sadhana-Acad. Proc. Eng. Sci., **37**(3), pp. 319–340.
[38] Pascual, B., and Adhikari, S., 2012, "Combined Parametric-Nonparametric Uncertainty Quantification Using Random Matrix Theory and Polynomial Chaos Expansion," Comput. Struct., **112–113**, pp. 364–379.
[39] Wiener, N., 1938, "The Homogeneous Chaos," Am. J. Math., **60**(4), pp. 897–936.
[40] Xiu, D., and Karniadakis, G. E., 2002, "The Wiener–Askey Polynomial Chaos for Stochastic Differential Equations," SIAM J. Sci. Comput., **24**(2), pp. 619–644.
[41] Hu, C., and Youn, B. D., 2010, "Adaptive-Sparse Polynomial Chaos Expansion for Reliability Analysis and Design of Complex Engineering Systems," Struct. Multidiscip. Optim., **43**(3), pp. 419–442.
[42] Wei, D., Cui, Z., and Chen, J., 2008, "Uncertainty Quantification Using Polynomial Chaos Expansion With Points of Monomial Cubature Rules," Comput. Struct., **86**(23–24), pp. 2102–2108.
[43] Goswami, S., and Chakraborty, S., 2016, "An Efficient Adaptive Response Surface Method for Reliability Analysis of Structures," Struct. Saf., **60**, pp. 56–66.
[44] Kang, S.-C., Koh, H.-M., and Choo, J. F., 2010, "An Efficient Response Surface Method Using Moving Least Squares Approximation for Structural Reliability Analysis," Probab. Eng. Mech., **25**(4), pp. 365–371.
[45] Li, J., Wang, H., and Kim, N. H., 2012, "Doubly Weighted Moving Least Squares and Its Application to Structural Reliability Analysis," Struct. Multidiscip. Optim., **46**(1), pp. 69–82.
[46] Taflanidis, A. A., and Cheung, S.-H., 2012, "Stochastic Sampling Using Moving Least Squares Response Surface Approximations," Probab. Eng. Mech., **28**, pp. 216–224.
[47] Xiong, F., Greene, S., Chen, W., Xiong, Y., and Yang, S., 2009, "A New Sparse Grid Based Method for Uncertainty Propagation," Struct. Multidiscip. Optim., **41**(3), pp. 335–349.

[48] Hu, C., and Youn, B. D., 2011, "An Asymmetric Dimension-Adaptive Tensor-Product Method for Reliability Analysis," Struct. Saf., **33**(3), pp. 218–231.
[49] Bollig, E. F., Flyer, N., and Erlebacher, G., 2012, "Solution to PDEs Using Radial Basis Function Finite-Differences (RBF-FD) on Multiple GPUs," J. Comput. Phys., **231**(21), pp. 7133–7151.
[50] Deng, J., Gu, D., Li, X., and Yue, Z. Q., 2005, "Structural Reliability Analysis for Implicit Performance Functions Using Artificial Neural Network," Struct. Saf., **27**(1), pp. 25–48.
[51] Jamshidi, A. A., and Kirby, M. J., 2010, "Skew-Radial Basis Function Expansions for Empirical Modeling," SIAM J. Sci. Comput., **31**(6), pp. 4715–4743.
[52] Lazzaro, D., and Montefusco, L. B., 2002, "Radial Basis Functions for the Multivariate Interpolation of Large Scattered Data Sets," J. Comput. Appl. Math., **140**(1–2), pp. 521–536.
[53] Marchi, S. D., and Santin, G., 2013, "A New Stable Basis for Radial Basis Function Interpolation," J. Comput. Appl. Math., **253**, pp. 1–13.
[54] Chakraborty, S., and Chowdhury, R., 2016, "Assessment of Polynomial Correlated Function Expansion for High-Fidelity Structural Reliability Analysis," Struct. Saf., **59**, pp. 9–19.
[55] Chakraborty, S., and Chowdhury, R., 2015, "A Semi-Analytical Framework for Structural Reliability Analysis," Comput. Methods Appl. Mech. Eng., **289**(1), pp. 475–497.
[56] Chakraborty, S., and Chowdhury, R., 2016, "Modelling Uncertainty in Incompressible Flow Simulation Using Galerkin Based Generalised ANOVA," Comput. Phys. Commun., **208**, pp. 73–91.
[57] Chakraborty, S., and Chowdhury, R., 2016, "Sequential Experimental Design Based Generalised ANOVA," J. Comput. Phys., **317**, pp. 15–32.
[58] Chakraborty, S., Mandal, B., Chowdhury, R., and Chakrabarti, A., 2016, "Stochastic Free Vibration Analysis of Laminated Composite Plates Using Polynomial Correlated Function Expansion," Compos. Struct., **135**, pp. 236–249.
[59] Chakraborty, S., and Chowdhury, R., 2015, "Polynomial Correlated Function Expansion for Nonlinear Stochastic Dynamic Analysis," J. Eng. Mech., **141**(3), p. 04014132.
[60] Chakraborty, S., and Chowdhury, R., 2017, "Polynomial Correlated Function Expansion," *Modeling and Simulation Techniques in Structural Engineering*, IGI Global, Hershey, PA, pp. 348–373.
[61] Hooker, G., 2007, "Generalized Functional ANOVA Diagnostics for High-Dimensional Functions of Dependent Variables," J. Comput. Graphical Stat., **16**(3), pp. 709–732.
[62] Li, G., and Rabitz, H., 2012, "General Formulation of HDMR Component Functions With Independent and Correlated Variables," J. Math. Chem., **50**(1), pp. 99–130.
[63] Biswas, S., Kundu, S., and Das, S., 2015, "Inducing Niching Behavior in Differential Evolution Through Local Information Sharing," IEEE Trans. Evol. Comput., **19**(2), pp. 246–263.
[64] Das, S., and Suganthan, P. N., 2011, "Differential Evolution: A Survey of the State-of-the-Art," IEEE Trans. Evol. Comput., **15**(1), pp. 4–31.
[65] Storn, R., and Price, K., 1997, "Differential Evolution–A Simple and Efficient Heuristic for Global Optimization Over Continuous Spaces," J. Global Optim., **11**, pp. 341–359.
[66] Stutz, L. T., Tenenbaum, R. A., and Correa, R. A. P., 2015, "The Differential Evolution Method Applied to Continuum Damage Identification Via Flexibility Matrix," J. Sound Vib., **345**, pp. 86–102.
[67] Beyer, H. G., and Sendhoff, B., 2007, "Robust Optimization–A Comprehensive Survey," Comput. Methods Appl. Mech. Eng., **196**(33–34), pp. 3190–3218.
[68] Chen, W., Allen, J., Tsui, K., and Mistree, F., 1996, "Procedure for Robust Design: Minimizing Variations Caused by Noise Factors and Control Factors," ASME J. Mech. Des., **118**(4), pp. 478–485.
[69] Park, G., Lee, T., Kwon, H., and Hwang, K., 2006, "Robust Design: An Overview," AIAA J., **44**(1), pp. 181–191.
[70] Schuëller, G., and Jensen, H., 2008, "Computational Methods in Optimization Considering Uncertainties An Overview," Comput. Methods Appl. Mech. Eng., **198**(1), pp. 2–13.
[71] De Groot, M., 1970, *Optimal Statistical Decisions*, McGraw-Hill, New York.
[72] Taguchi, G., 1986, *Quality Engineering Through Design Optimization*, Krauss International Publications, White Plains, NY.
[73] Doltsinis, I., and Kang, Z., 2004, "Robust Design of Structures Using Optimization Methods," Comput. Methods Appl. Mech. Eng., **193**(23–26), pp. 2221–2237.
[74] Chakraborty, S., and Chowdhury, R., 2015, "Multivariate Function Approximations Using D-MORPH Algorithm," Appl. Math. Model., **39**(23–24), pp. 7155–7180.
[75] Alis, O. F., and Rabitz, H., 2001, "Efficient Implementation of High Dimensional Model Representations," J. Math. Chem., **29**(2), pp. 127–142.
[76] Rabitz, H., and Ali, Ö. F., 1999, "General Foundations of High Dimensional Model Representations," J. Math. Chem., **25**(2–3), pp. 197–233.
[77] Sobol, I. M., 1993, "Sensitivity Estimates for Nonlinear Mathematical Models," Math. Model., **2**(1), pp. 112–118.
[78] Li, G., Rey-de Castro, R., and Rabitz, H., 2012, "D-MORPH Regression for Modeling With Fewer Unknown Parameters Than Observation Data," J. Math. Chem., **50**(7), pp. 1747–1764.
[79] Li, G., and Rabitz, H., 2010, "D-MORPH Regression: Application to Modeling With Unknown Parameters More Than Observation Data," J. Math. Chem., **48**(4), pp. 1010–1035.
[80] Rao, C., and Mitra, S. K., 1971, *Generalized Inverse of Matrix and Its Applications*, Wiley, New York.
[81] Ma, X., and Zabaras, N., 2010, "An Adaptive High-Dimensional Stochastic Model Representation Technique for the Solution of Stochastic Partial Differential Equations," J. Comput. Phys., **229**(10), pp. 3884–3915.
[82] Ren, X., and Rahman, S., 2013, "Robust Design Optimization by Polynomial Dimensional Decomposition," Struct. Multidiscip. Optim., **48**(1), pp. 127–148.
[83] Heiss, F., and Winschel, V., 2008, "Likelihood Approximation by Numerical Integration on Sparse Grids," J. Econometrics, **144**(1), pp. 62–80.
[84] Lee, I., Choi, K., Du, L., and Gorsich, D., 2008, "Dimension Reduction Method for Reliability-Based Robust Design Optimization," Comput. Struct., **86**(13–14), pp. 1550–1562.
[85] Bratley, P., and Fox, B. L., 1988, "Implementing Sobols Quasirandom Sequence Generator," ACM Trans. Math. Software, **14**(1), pp. 88–100.
[86] Sobol, I. M., 1976, "Uniformly Distributed Sequences With an Additional Uniform Property," USSR Comput. Math. Math. Phys., **16**(5), pp. 236–242.